Ensembles of global ocean analyses for seasonal climate prediction: impact of temperature assimilation

Philippe Rogel*, Anthony T. Weaver, Nicolas Daget, Sophie Ricci, Eric Machu (1)

Centre Européen de Recherche et de Formation Avancée en Calcul Scientifique
CERFACS/SUC URA 1875, Toulouse, France

(1) Now at Centre de Recherches Halieutiques Mediterranéenne et tropicale, Sète, France

Submitted to Tellus A, Demeter special issue

Revised version: September 27, 2004

* Corresponding author
Email: rogel@cerfacs.fr

Abstract

Two sets of ensembles of ocean initial conditions for seasonal climate prediction have been constructed following a strategy that preserves the dynamical balance of the ocean. One set has been constructed by perturbing the wind stress and sea surface temperature forcing of an ocean model. The other set is constructed by assimilating perturbed in situ temperature data using a fully multivariate three dimensional variational system, in addition to using the perturbed forcing. Ensemble statistics are computed for the period 1990 to 1999.

The ensemble mean temperature has a significant subsurface cold bias when no data are assimilated, indicating that some part of the DEMETER hindcast systematic error may be explained by the way the ensembles are generated. Constraining the temperature through data assimilation contributes to a reduction in this subsurface bias.

The dispersion of the initial conditions is supposed to sample the uncertainty associated with the ocean initial state estimate. Therefore, a smaller spread in the assimilation case than in the forced only case is consistent with the idea that ocean uncertainty has been reduced by constraining the ocean state through data assimilation. However, comparing ensemble spread and innovation statistics suggests that ocean uncertainty may be underestimated by the ensemble method in the assimilated case. It is also shown that wind stress perturbations mainly control the spread amplitude in the non-assimilated case, but that perturbed sub-surface temperature observations have a stronger relative impact in the assimilation case.

1. Introduction

At seasonal to interannual time scales, the upper ocean thermal and dynamical inertia is one major source of climate predictability. For seasonal climate prediction, it is therefore highly desirable to initialise as accurately as possible the ocean component of a coupled ocean-atmosphere forecast system. Several studies have shown that the use of ocean data assimilation to produce initial conditions (ICs) has a positive impact on the skill of coupled ocean-atmosphere predictions of tropical climate variations (Ji and Leetma, 1997; Rosati et al., 1997; Segschneider et al., 2000; Alves et al., 2004). The skill improvement may depend on the quality of the data (wind stress, heat and fresh water fluxes, sea surface temperature) used to force the ocean model (Alves et al., 2004), or on the nature of the assimilated ocean observations (Segschneider et al., 2002).

The uncertainty associated with ocean ICs should be exploited in order to estimate the uncertainty of a given forecast. An innovative idea of the DEMETER project (Palmer et al., 2004) was to use error sampling of the ocean ICs as a way to generate ensembles of coupled seasonal integrations. This was done by applying a perturbation technique to one ocean IC in order to derive as many ocean state estimates as ensemble members needed for the forecast. However, few studies have investigated in detail the impact of such an ensemble generation technique on the forecasts.

In a recent paper, Vialard et al. (2004) have tested several ensemble generation techniques that sample errors in the initial conditions induced by uncertainties in wind stress and sea surface temperature (SST), and errors in the atmospheric model physics. One of these techniques, which uses perturbations of wind stress forcing and upper ocean temperature, is used in the operational seasonal forecast system (system 2) of the European Centre for Medium-range Weather Forecasts (ECMWF; see Anderson et al., 2003). Vialard et al. (2004) found that none of the methods used has a noticeable impact on the forecast ensemble spread at lead times of 3 to 6 months, suggesting that coupled model error is an appreciable factor for the mean coupled state as well as the ensemble spread. An hypothesis can be made that some part of the coupled model error, especially during the first days of coupled integration, may come from imbalances, not only between the ocean and atmospheric initial states, but also in the ocean state itself as inferred by the ensemble generation technique. In particular, the introduction of upper ocean temperature perturbations in most ensemble members does not preserve the mixed layer properties. Another result of Vialard et al. (2004) shows that ocean ICs obtained through assimilation of *in situ* temperature data lead systematically, and possibly excessively, to smaller forecast ensemble spread. This suggests that there is room for improving the ensemble generation method when ocean data are assimilated.

In this paper, an ensemble generation strategy is presented, which is designed to address the aforementioned problems. The ensemble generation method uses the same sets of perturbed wind stress and SST as Vialard et al. (2004), but has been adapted to conserve dynamical properties of the upper ocean. This technique is extended to the case where *in situ* temperature data are assimilated. In particular, temperature observation perturbations are constructed in a way that is consistent with the overlying SST perturbations. How this procedure is able to modify both the ensemble mean and spread of the ocean ICs is investigated. Typical sets of ocean ICs (i.e., ensembles of instantaneous ocean states) produced for DEMETER seasonal hindcast experiments are examined. Our focus will be on the tropical oceans which are the primary sources for seasonal climate predictability. The paper is organised as follows. In section 2, the system used to obtain ensembles of ocean ICs, including the model, data assimilation system, and perturbation technique, is described, and the impact of data assimilation on the mean state and variability of the ocean ICs is briefly presented. Section 3 discusses how the ensemble generation impacts the mean bias and spread of ocean ICs. Finally, section 4 provides a summary and discussion.

2. The global ocean ensemble analysis system

2.1 Model and forcing

The ocean general circulation model (OGCM) used in this study is the global, free surface version of OPA (Madec et al., 1998; Roullet and Madec, 2000). It solves the primitive equations for horizontal currents, potential temperature, salinity, and free surface elevation in a horizontal z-curvilinear coordinate system. This global configuration has an average resolution of 2° in longitude and 1.5° in latitude, the latter resolution being increased to 0.5° in the equatorial band. There are 31 vertical levels, of which 10 are in the top 100 metres, to ensure that there is increased resolution in the mixed layer and thermocline in the tropical regions.

Daily wind stress, heat and fresh water fluxes, and SST are used to force the model. These are derived from ECMWF forecasts issued twice a day from the ERA40[†] re-analysis of atmospheric variables. More precisely, daily wind stress fields have been extracted from 0 to 12 hour ERA40 atmospheric forecasts, while heat and fresh water fluxes have been extracted from 12 to 24 hour forecasts, in order to avoid erroneous fluxes due to the model spin up.

[†] Information on the ECMWF Re-Analysis of 40 years can be found at http://www.ecmwf.int/research/era.

Daily SST analyses from ERA40 are used, which are derived from the weekly analyses from NCEP‡. The strength of the restoring term towards the daily SST fields has been set at -200 $W/m^2/°C$. This strategy was defined jointly in the DEMETER project in order to force the ocean model's SST to be as close as possible to the observations before performing a coupled forecast. This has implications for the perturbation strategy described below.

2.2 The assimilation system and the assimilated data set

The assimilation system used for the OPA model is an updated version of the three dimensional variational (3D-Var) system described in Weaver et al. (2003) and Ricci et al. (2004). 3D-Var is defined by the minimisation of a cost function comprising two terms: an observation term (J_o) which measures the squared misfits between the observations and their model equivalent, weighted by the inverse of an estimate of the observation error covariance matrix; and a background term (J_b) which measures the squared misfit of the unknown model state to the background state (in our case the model state before assimilation), weighted by the inverse of an estimate of the background error covariance matrix. The purpose of this paper is not to document the details of the 3D-Var system. For this reason, only an outline of the main differences between the 3D-Var system used here and that used by Weaver et al. (2003) and Ricci et al. (2004) is presented below.

In the studies of Weaver et al. (2003) and Ricci et al. (2004), the configuration was limited to the tropical Pacific Ocean and employed a rigid-lid version of OPA, whereas in the current study the configuration covers the global ocean and employs a free-surface version of OPA. This required making two important changes to the 3D-Var system. First, with the

‡ Available at http://www.cdc.noaa.gov/cdc/data.noaa.oisst.v2.html.

introduction of a free surface, sea surface height becomes an additional component of the model state vector and, unlike in the rigid-lid model, the vertical integral of the horizontal velocity is no longer required to be non-divergent. The full state vector of the free surface model, which is to be estimated from 3D-Var, thus comprises temperature, salinity, horizontal velocity and sea surface height. Second, to account for the non-geographical grid in the global model, substantial modifications needed to be made to the observation operator (the grid-point search algorithm as well as the interpolation method) in order to be able to compute the model temperature at measurement locations on in situ profiles. The observation operator used in this study consists of bilinear interpolation along model levels and spline interpolation between model levels.

The potential for 3D-Var to extract information from observations and to produce ocean analyses that are both smooth and dynamically balanced is, to a large extent, governed by the formulation of the J_b term. The J_b term used here is similar to the one used in Ricci et al. (2004), with some important extensions. First, following Behringer et al. (1998) and Alves et al. (2004), the background-error variances have been made dependent on the vertical gradient of background temperature in order to focus the largest variances in regions where thermal variability is large. Within each vertical profile, the variances are normalized such that the maximum variance is $(1.5°C)^2$ at the level of maximum vertical gradient. Second, the J_b term has been made fully multivariate using a linear balance operator. In addition to the temperature-salinity constraints described by Ricci et al. (2004), the balance operator includes hydrostatic, dynamic height and geostrophic constraints in order to link temperature and salinity with sea surface height and horizontal currents. Geostrophic adjustments are included near the equator by employing a β-plane approximation similar to what is done for adjusting velocity in the ECMWF ocean analysis system (Balmaseda, 2004). In this paper, the effect of all these extensions on the general performance of the system will not be discussed. However, it should be emphasized that they do play an important role in producing balanced perturbations in the ensemble generation technique.

The 3D-Var analysis is performed using observations within a 10-day assimilation window. Another characteristic of the system important for the following is the method used to introduce the analysis increments in the model. This is done using the so-called Incremental Analysis Update method (Bloom et al. 1996), in which the increment is applied smoothly and progressively via a forcing term in the general trend equations of the model. This procedure is designed to preserve realistic balances in the model by reducing the assimilation 'shock'.

In the experiments described below, the assimilated observations are global *in situ* temperature measurements from the Global Temperature and Salinity Pilot Project (GTSPP) of the National Oceanographic Data Center. This is the same basic data-set used by Weaver et al. (2003), Vialard et al. (2003) and Ricci et al. (2004), but with additional GTSPP data included for years 1990 to 1992. This data-set includes measurements mainly from TAO moorings and XBTs, plus a limited number of CTD casts and drifting buoys. A manual quality control procedure was used to remove suspect data. The observation errors are assumed to be uncorrelated and to have error variance equal to $(1°C)^2$.

2.3 Unperturbed experiments

Two unperturbed experiments have been conducted for the period November 1986 to February 1999. In the following discussion, only years from 1990 to 1999 are considered in order to avoid the first 3 "spin up" years of the data assimilation.

The first experiment (denoted FORCED hereafter) has no data assimilation. The OPA global model was spun up from rest and Levitus et al. (1994) temperature and salinity, using a blended climatology of ERS and *in situ* (mostly TAO) observed winds, and heat and fresh water fluxes derived from ERA15 and Xie and Arkin (1996) precipitation analyses. After a two-year spin up, during which the model remained close to climatology, the model was forced with ERA40 daily fluxes, wind stresses, and restored towards ERA40 daily SST from November 1, 1986 onwards.

In the second experiment (denoted 3DVAR hereafter), *in situ* temperature observations are assimilated using the 3D-Var system which is cycled over the same period as in FORCED, starting from the same spin up state as in FORCED.

As stated above, only instantaneous ocean states used as ICs for coupled seasonal hindcasts, obtained for the first day of February, May, August and November, are considered here. They would constitute the ocean ICs for coupled models using the OPA OGCM. Figure 1 shows an equatorial vertical section of the standard deviation of interannual temperature anomalies in both FORCED and 3DVAR. The effect of assimilating *in situ* temperature is to significantly increase the temperature variability in the model. In the tropical Pacific, the pattern is qualitatively similar in FORCED and 3DVAR, but the amplitude is increased in the latter, partly because the mean temperature state has a steeper thermocline gradient. There is a spectacular change in the tropical Atlantic and, to a lesser extent, in the tropical Indian oceans.

As shown in Ricci et al. (2004), the J_b model formulation is designed to include physical constraints so that non-assimilated variables such as salinity and currents are corrected when only single-variable information (temperature) is assimilated. In summary, the effect of the global 3D-Var assimilation is to improve the mean state and variability of the ocean subsurface. Note that the maps shown here, as well as most maps shown in the following, are somewhat noisy, because only instantaneous fields have been considered.

2.4 The perturbation technique

This section describes how perturbation techniques have been developed for both the FORCED and 3DVAR experiments. They use sets of daily wind stress and three-monthly SST perturbations common to all DEMETER participants and similar to those used in Vialard et al. (2004). Those sets of perturbations have been constructed from statistics of differences between various operational estimates of wind stress and SST. Ensembles of 8 perturbed ocean ICs have been constructed for the beginning of each season, from February 1990 to February 1999, giving a total of 288 ocean initial states, for each of the FORCED and 3DVAR experiments. The perturbation procedures have been defined in order to preserve as much as possible the ocean dynamics during the perturbation procedure. In contrast, the temperature perturbation procedure used in the ECMWF system (described in Vialard et al., 2004) and by other DEMETER participants consists of changing the upper ocean temperature with the full perturbation at the surface, and ramping it to zero at 40 metres. This is done without preserving any other ocean properties, especially in the mixed layer.

2.4.1 Forced perturbation technique

The ocean ICs constructed in the FORCED case were used for two of the DEMETER hindcast models (denoted CERFACS and LODYC in Palmer et al., 2004). The strategy used to produce perturbed ensembles of ocean ICs is summarised in Figure 2a. In the FORCED case, every three months, an IC from the unperturbed forced ocean run is used to start two wind-stress-perturbed forced runs (using positive and negative daily wind stress perturbations). Fourteen days before the target date T0, four SST perturbations (again provided by ECMWF) are added to and subtracted from the restored SST. The perturbations are introduced progressively using a linear weighting function with amplitude zero at day T0–14, and amplitude one at day T0-7; between T0-7 and T0, the full perturbation is applied. Compared to the perturbation procedure applied by other DEMETER participants (e.g. running wind stress perturbed experiments over long periods, and applying SST perturbations instantaneously), restarting every three months from unperturbed experiments ensures that the long term climate drift in the ocean is the same for all ocean ICs. On the other hand, wind stress perturbations have less time to perturb the ocean, thus potentially leading to a smaller spread inside the IC ensemble. Restoring the model towards perturbed SSTs keeps the water column properties (salinity, currents, mixing) internally consistent with the model equations. In addition, the restoring timescale associated with a flux "correction" term of -200 $W/m^2/°C$ is about 7 days for a 50-metre-deep mixed layer, so that the model surface perturbation in temperature after 14 days is of the same order of magnitude as the SST perturbation itself. The spread due to SST perturbations is thus very close to the root mean squared difference of the SST perturbations. Note also that the choice of combining both sources of perturbations, which was decided in common within the DEMETER project, is not symmetrical for each ensemble. However, on average over a sufficiently long period, one can consider that the statistics of the forcing perturbations are symmetrical.

2.4.2 Perturbations of 3D-Var analyses

In 3DVAR, in addition to the forcing perturbation as described above, other perturbations are added to the system to produce ensembles of ocean initial conditions in the presence of data assimilation. In order to preserve as closely as possible the same procedure for perturbing the ocean state as described above, sets of perturbed observations have been constructed by horizontally interpolating the SST perturbations to the location of the observed *in situ* profiles. The perturbations are extrapolated from the subsurface to the bottom of the mixed layer (as defined from the observed profile itself by a temperature criterion) and smoothly reduced to zero beneath. Thus, as seen in Figure 2b, the shape of the mixed layer is preserved. Perturbing observations also avoids any inconsistencies between the perturbed SST and the assimilated observed temperature in the perturbation process. The observation perturbation has been applied smoothly in time, consistently with what was done for SST in the unassimilated case.

3 Impact of data assimilation on the ocean initial conditions ensemble statistics

3.1 Impact on the bias

Since the choice was to perturb the ocean ICs through wind stress forcing and the SST restoring term, there is no control on the effect of this procedure on statistics of the ensembles of ocean states thus constructed. In particular, there is no guarantee that the ensemble mean state is not biased with respect to the unperturbed ocean IC, in some sense the most realistic estimate of the ocean state. This is verified in Figure 3, which is an estimate of the bias introduced by the ensemble generation methods in FORCED and 3DVAR. This bias has been estimated as the averaged difference between all ocean member states and the unperturbed ocean states. The average has been computed over all seasons of the entire 1990 to 1999 period.

The bias introduced by the ensemble generation method is not negligible in FORCED. It is close to zero in the surface layer of the model, as can be seen from Figure 3a, and from a horizontal map of the same field (not shown). This is a consequence of the direct control of the model SST by the very strong relaxation term towards which perturbations have a zero average. However, the indirect response to both types of perturbations occurs in the subsurface. A large scale negative bias, with core amplitude locally exceeding -0.15°C at depths between 50m and 100m is clearly visible in the tropical Pacific. A positive bias appears at depth near the coast of Peru, with a maximum exceeding 0.35 °C near 50 m. A large scale positive bias can also be identified in the warm-pool region between 100 m and 150 m, though its amplitude is weaker. The horizontal extension of this bias is symmetric with respect to the equator. It is also present at all the seasons (not shown). In the tropical Atlantic ocean, a similar though less intense pattern can be observed. In the Indian ocean, one can see the same kind of pattern, however, the amplitude is so weak that it has no real significance.

Figure 3b shows the same bias estimate, but for 3DVAR. In the central tropical Pacific, the negative large-scale bias, close to the surface, has been substantially reduced, as well as the warm bias close to the coast of Peru. In general, the bias introduced in that case has patterns confined in the region of the main thermocline temperature gradient. The largest of these patterns is a cold/warm vertical dipole close to the date line, between 100 m and 150 m. The positive anomaly may indicate that, on average, the thermocline is deepened in this area by the ensemble generation technique. In the eastern part of the basin, negative, less intense anomalies can be observed, that could be associated with a shallower thermocline depth. In the tropical Atlantic and Indian oceans, the mean bias is mainly cold and located in the eastern part of the basin. Note that the bias in the Indian ocean is almost the same as in Figure 3a for FORCED. This is probably due to poorer observation coverage in this region.

The biases shown in Figure 3 reflect in some sense the non-symmetric (non-linear) response of the ocean to normally distributed forcing perturbations. In FORCED, both sources of perturbation may have nonlinear effects leading to a subsurface bias of the ensemble mean. For example, one can easily conceive that in regions where the relaxation is towards temperatures colder than ERA40 (i.e. where SST perturbations are negative), the induced perturbation will have a tendency to propagate at depth, in order to preserve the water column stability. In contrast, a perturbation towards warmer temperature will increase the stratification and will not propagate downward. The net effect should be a cold bias in the subsurface, and the negative bias observed in the Pacific near 50 m in Figure 3a could reflect this non-linear response. As for the wind stress perturbation, it is clear that a westward (an eastward) trade wind perturbation will tend to steepen (flatten) the thermocline. However, it can be anticipated that the steepening will have less amplitude than the flattening, so that the net effect should be a dipole (negative in the west, positive in the east) associated with a mean flatter-than-unperturbed thermocline slope. The warm bias near the Peru coast in Figure 3a could thus be interpreted as a non-linear influence of the wind stress perturbations.

In 3DVAR, the interpretation is more complicated. On the one hand, temperature observation perturbations are constructed so that their effect in the subsurface is not biased in the mixed layer. This may explain why the negative bias of Figure 3a in the Pacific near 50 m is reduced. On the other hand, since observations are not perturbed deeper than 50 m, the thermocline depth and temperature gradient should be entirely controlled by data assimilation where data coverage is dense enough, and therefore the bias introduced by the wind stress perturbations should be substantially reduced as well. This is the case in the eastern part of the basin. However, the strong cold/warm dipole is a new feature introduced by the data assimilation and perturbation procedures. Some nonlinear effects of the background-state-dependent J_b formulations, such as the background error variance parameterisation based on the vertical temperature gradient, could play an important role in this region, where indeed the vertical gradient is strong.

3.2 Impact on the ensemble spread

3.2.1 Mean spread

As presented earlier, the goal of constructing ensembles is to sample ocean state uncertainty. To estimate this uncertainty, Figure 4 shows a vertical section at the equator of the mean spread of the ocean initial conditions averaged over all seasons of the period 1990 to 1999, in FORCED and 3DVAR. In FORCED (Figure 4a), the spread is of the order of 0.2°C to 0.3°C at the surface of the western parts of the three ocean basins, and 0.4°C in the eastern parts. As for the bias, the mean spread is directly controlled by the strong restoring term towards perturbed SST. At depth, the spread is maximum along the mean position of the thermocline temperature gradient, with a maximum value of 1.6°C in the eastern part of the basin at a depth of 50 m. The same picture can be drawn for the other tropical basins, except that the amplitude is weaker (maxima of 0.8°C in the Atlantic, 1.0°C in the Indian) and at different depths (40 m for the Atlantic, 100 m for the Indian). The seasonal cycle in the tropical Pacific (not shown here) is such that the spread is maximum in May (though close to February values), and minimum in August. This is not the case for the other oceans: it is maximum in May but minimum in February in the Atlantic, whereas it is maximum in August and minimum in February in the Indian. Another general feature lies in the fact that the mean spread has a much larger amplitude than the mean ensemble bias discussed in section 3.1. This the case in all oceans and at all depths, and is also true for 3DVAR.

In 3DVAR (Figure 4b), while the surface temperature spread amplitude is somewhat similar to FORCED in the surface layer, the same kind of patterns as Figure 3b can be observed at subsurface, with a maximum amplitude of the spread occurring along the mean position of the thermocline. However, the values are typically much weaker than in FORCED. Maximum values of the spread in all oceans are of the order of 0.7°C. In general, the spread pattern in the Atlantic and Indian oceans is not substantially modified with respect to FORCED. Another impact of the temperature assimilation on the spread is that no seasonal cycle in the spread can be clearly identified in the tropical Pacific.

In terms of variance of the perturbed ocean ICs, which is supposed to be consistent with the error variance associated with the unperturbed IC, we can estimate from Figure 1 that, in FORCED, the dispersion of the ensemble amounts to about 25% of the variance of the interannual anomalies in the surface layers, and 40% at the thermocline level. The impact of data assimilation is to reduce this ratio to about 10% near the surface, and 5% at the thermocline level. This is the result of both increased variability in the model and a decrease of the spread. The implications that this may have for further development of the ensemble technique, as well as for coupled forecasts, are discussed in section 4.

3.2.2 Linear response to perturbations

In order to analyse how the perturbations impact the ocean state, the mean linear response of the ocean to the perturbation procedure is shown in the following. This linear response has been estimated as half the difference of the "positively" perturbed ocean states (i.e. numbered 1+ to 4+ in Figure 2a) and the "negatively" perturbed states. This is shown in Figure 5 for both FORCED and 3DVAR cases.

In the FORCED case (Figure 5a), the response is to create a dipole in the tropical Pacific, with cores of anomalies at 50 m around 100°W, and 150 m at the dateline. The amplitude of anomalies is of the order of 0.35°C, with local larger values. This large scale subsurface response is consistent with a mean change of thermocline slope, shallower in the east, deeper in the warm-pool region. In both tropical Atlantic and Indian oceans, a similar pattern can be observed, however reversed, with a thermocline shallower in the west and deeper in the east.

Figure 5b shows the same response estimate, but for the 3DVAR case. In the tropical Pacific, the large scale response has been substantially reduced. A smaller effect on the slope of the thermocline can be observed, however with the reverse sign, indicating a shallower thermocline in the central and west Pacific, and deeper in the east. However, as noted above, since the first order effect of *in situ* temperature assimilation is to sharpen the thermocline gradient, a small change in the thermocline depth can induce a temperature change stronger than in the Forced case. Note that such a change in the mean response of the ocean to perturbations is not observed in the other tropical oceans.

3.2.3 Separating impacts from wind and temperature perturbations

Figures 4 and 5 measure the average impact of all sources of perturbation applied to the ocean. Though the perturbations are applied simultaneously, it is possible to have some idea of the separate impact of perturbing temperature on the one hand, and wind stress on the other. To do this, we have estimated the IC mean spread by considering two subsets of the ensembles. Ensemble members numbered 4+ and 1- in Figure 2 are only temperature perturbed, whereas ensemble members 2+ and 2- are perturbed by both temperature and wind stress. The variance of those two sub-ensembles can be compared, since they have the same size, and thus can provide some insight on the relative influence of temperature perturbations. This is shown in Figures 6 and 7. By comparing both figures for each case (FORCED and 3DVAR) it appears that the temperature perturbation accounts for up to 25% of the total variance of the ICs in the surface layers in both cases. However, at the thermocline level, the temperature perturbation accounts for up to 30% of the total variance of the ICs in FORCED, and 45% in 3DVAR. This means that the temperature perturbation has more importance in the case where temperature data are assimilated. This justifies the perturbed ocean observations approach. Indeed, in the case where temperature observations would not have been perturbed, data assimilation would have strongly controlled the subsurface temperature field and thus reduced the spread even more.

4 Summary and discussion

In this study, an ocean analysis system based on an OGCM has been used to define a pragmatic ensemble generation method. Two sets of ensembles of ocean ICs have been produced for the period 1990-1999, with the aim of initialising coupled seasonal hindcast experiments. One set is produced by applying perturbed SST and wind stress forcing fields to the ocean model, while the other set is produced by assimilating perturbed *in situ* temperature observations, in addition to using the perturbed forcing fields.

The ocean mean state and variability is significantly improved by temperature data assimilation. The perturbation procedure has been designed in order to preserve as much as possible realistic dynamical and physical balances in the ocean model, especially in the upper and main thermocline layers, where the ocean memory is crucial for seasonal climate predictability. This preservation is necessary to minimize the adverse effects of ocean "spin up" at the beginning of the coupled integration.

The ensemble generation in FORCED has a non-zero mean impact on the ocean ICs. A cold subsurface bias is thus induced in the Pacific ocean, reflecting the nonlinear response of the ocean model to temperature perturbations. This bias is somewhat corrected by temperature assimilation. In that case, a different systematic nonlinear response is observed, confined deeper, near the thermocline maximum temperature gradient.

The mean bias introduced in FORCED, though having smaller amplitude than the mean spread of the ensemble, may have an impact on subsequent ensembles of coupled integrations. The cold subsurface bias may initiate a coupled feedback involving stronger easterlies. Indeed, such a cold bias can be observed in verification results of the DEMETER hindcasts of the first month. For 3DVAR initialised hindcasts, this effect on the coupled integrations should be reduced.

The mean subsurface spread of the ocean ICs is shown to be dramatically impacted by data assimilation. This spread, which is mainly due to the linear response to wind stress perturbations as a change in the thermocline slope in FORCED, is reduced by data assimilation, and the sign of the response is reversed. In order to assess the impact of perturbing the observations on the mean spread, a sensitivity experiment where unperturbed observations are assimilated was carried out. This experiment was limited to the year 1990 (9 members for each season), during which no significant interannual signal was observed in the Pacific. In the tropics, comparing the spread of this experiment to the 1990 equivalent of Figure 4b (not shown here) clearly demonstrates that the effect of perturbing the observations is to increase the spread in the upper layers of the model. In particular, the spread may be increased on average by 30% to 40% down to the main thermocline depth, however with regional differences. In this particular case, the spread increase is largest (up to 100% locally) in the tropical central Pacific down to 150 metres, in the tropical western Atlantic, and in the tropical central Indian oceans.

If the mean spread of the present ensembles of ocean ICs are compared to those of Vialard et al. (2004, see their Figure 2), one can see that the order of magnitude is comparable in both non-assimilated and assimilated cases, and especially in the surface layers. The two main differences introduced by the present method (e.g. restarting the wind stress perturbation every three months, and perturbing SST through the restoring term) thus do not seem to reduce the temperature spread. However, the spread is consistently extended to all model variables, so that no imbalances in the ocean state are present at the first time step of the subsequent coupled experiment.

As already emphasized at the beginning, the ensemble generation strategy is designed to sample the ocean state uncertainty. One way of validating whether error estimates through this method are realistic is to compare this approach to the more classical model/data comparison. Such statistics can be obtained from the model/data misfits (also called innovations) computed by the data assimilation system itself. Of course, a comparison with the ensemble method is possible only in places of the ocean where observations are sufficient. In this study, we have only considered TAO data, where temperature observations are collected every day over most of the period, at fixed mooring locations. Two examples are shown in Figure 8, based on data from equatorial moorings at 155°W and 95°W. Comparison with the ensemble spread in FORCED shows that the magnitude of the spread is of the same order as the innovation standard deviation, thus justifying a posteriori the background error standard deviation upper bound of 1.5°C. In 3DVAR, the innovation standard deviation is reduced, and it is thus consistent with the decrease of the spread of the 3DVAR ensemble. However, the spread of the 3DVAR ensembles is much less (spread maxima of 0.5°C and 0.7°C, innovation standard deviation maxima of 1.1°C and 1.5°C see Figure 8). This may indicate that the ensemble method probably underestimates the ocean state uncertainty in 3DVAR, though it would have been underestimated even more without perturbing the observations. This leaves possibilities for improving the ensemble generation method in the presence of data assimilation. One possibility is to design the observation perturbations so that they are consistent with the assumed observation error statistics used in the data assimilation system. This could be done for example using the square root of the observation error covariance matrix, and would have the advantage of producing perturbations not restricted to the mixed layer.

Acknowledgements:

The authors wish to thank the Seasonal Forecasting team at ECMWF for allowing the use of their GTSPP data base and sets of perturbations. The ERA40 project and CNRM/Météo-France provided the forcing fields. Financial support for this work was obtained from the EU-FP5 DEMETER project (EVK2-1999-00197). Additional support was provided by the French MERCATOR project and the EU-FP5 ENACT (EVK2-CT2001-00117) project.

References :

Anderson, D.L.T., T.N. Stockdale, M. Balmaseda, L. Ferranti, F. Vitart, P. Doblas-Reyes, R. Hagedorn, T. Jung, A. Vidard, A. Troccoli and T. Palmer, 2003. Comparison of the ECMWF seasonal forecast Systems 1 and 2, including the relative performance for the 1997/8 El Nino, ECMWF Tech Memo 404, Reading, UK.

Alves, O., M. Alonso Balmaseda, D.L.T. Anderson and T.N. Stockdale, 2004. Sensitivity of dynamical seasonal forecasts to ocean initial conditions. *Quart. J. Roy. Meteor. Soc.*, **130**, 647-667.

Balmaseda, M. A., 2004. Ocean data assimilation for seasonal forecasts. In *Proceedings of the ECMWF Seminar on" Recent developments in data assimilation for atmosphere and ocean", 8-12 September 2003*, ECMWF Proceedings series, Reading, UK, 476 pp, 301-325.

Behringer, D., M. Ji and A. Leetma, 1998. An improved coupled model for ENSO prediction and implications for ocean initialization. Part I: The ocean data assimilation system. *Mon. Wea. Rev.*, **126**, 1013-1021.

Bloom, S. C., L. L. Takacs, A.M. Da Silva and D. Levina, 1996. Data assimilation using incremental analysis updates. *Mon. Wea. Rev.*, **124**, 1256-1271.

Ji, M., and A. Leetma, 1997. Impact of data assimilation on ocean initialization and El Niño prediction. *Mon. Wea. Rev.*, **125**, 742-753.

Levitus, S., R. Burgett and T.P. Boyer, 1994. World Ocean Atlas. Salinity. *NOAA Atlas NESDIS 3, U.S. Department of Commerce*, **3**, 99pp.

Madec, G., P. Delecluse, M. Imbard and C. Lévy, 1998. OPA8.1 Ocean General Circulation Model reference manual. *Notes du Pôle de modélisation, Institut Pierre Simon Laplace (IPSL), France*, **11**, 91pp.

Palmer, T. N., A. Alessandri, U. Andersen, P. Cantelaube, M. Davey, P. Délécluse, M. Déqué, E. Diez, F. J. Doblas-Reyes, H. Feddersen, R. Graham, S. Gualdi, J.-F. Guérémy, R. Hagedorn, M. Hoshen, N. Keenlyside, M. Latif, A. Lazar, E. Maisonnave, V. Marletto, A. P. Morse, B. Orfila, P. Rogel, J.-M. Terres, M. C. Thomson, 2004. Development of a European Multi-Model Ensemble System for Seasonal to Inter-Annual Prediction (DEMETER). *Bull. Amer. Meteorol. Soc.*, **85**, 853-872.

Ricci, S., A. T. Weaver, J. Vialard, and P. Rogel, 2004. Incorporating state-dependent temperature-salinity constraints in the background-error covariance of variational ocean data assimilation. To appear in *Mon. Wea. Rev.*

Rosati, A., K. Miyakoda and R. Gudgel, 1997. The impact of ocean initial conditions on ENSO forecasting with a coupled model. *Mon. Wea. Rev.*, **125**, 754-772.

Roullet, G. and G. Madec, 2000. Salt conservation, free surface, and varying levels: a new formulation for ocean general circulation models. *J. Geophys. Res.*, **105**, 23297-23942.

Segschneider, J., D.L.T. Anderson, J. Vialard, M.A. Balmaseda and T.N. Stockdale, 2002. Initialization of seasonal forecasts assimilating sea level and temperature observations. *J. Climate*, **14**, 4292-4307.

Vialard, J., Weaver, A. T., Anderson, D. L. T. and P. Delecluse, 2003: Three- and four-dimensional variational assimilation with an ocean general circulation model of the tropical Pacific Ocean. Part 2: physical validation, *Mon. Wea. Rev.*, **131**, 1379-1395.

Vialard, J., F. Vitart, M. A. Balmaseda, T. N. Stockdale and D. L. T. Anderson, 2004. An ensemble generation method for seasonal forecasting with an ocean-atmosphere coupled model. To appear in *Mon. Wea. Rev*.

Weaver, A. T., and P. Courtier, 2001. Correlation modelling on the sphere using a generalized diffusion equation, *Quart. J. Roy. Meteor. Soc*., **127**, 1815-1846.

Weaver, A. T., J. Vialard and D. L. T. Anderson, 2003. Three- and four-dimensional variational assimilation with a general circulation model of the tropical Pacific Ocean. Part I: formulation, internal diagnostics and consistency checks. *Mon. Wea. Rev.*, **131**, 1360-1378.

Xie, P. and Arkin,P. A., 1996. Analyses of Global Monthly Precipitation Using Gauge Observations, Satellite Estimates, and Numerical Model Predictions. *J. Climate*, **9**, 840-858.

Figure Captions:

Figure 1: Equatorial section in the three oceans of the standard deviation of the interannual temperature anomalies, in a) FORCED, and b) 3DVAR. Isocontour interval is 0.2°C.

Figure 2: a) Schematic diagram of the ocean perturbation procedure in FORCED, and in 3DVAR (use of perturbed observations); b) example of perturbed observed temperature profiles in the tropical ocean; the central line is the original observed profile, bounded by positively and negatively perturbed profiles in the mixed layer.

Figure 3: Equatorial section of the mean bias introduced by the ensemble generation method in a) FORCED, and b) 3DVAR. Isocontour interval is 0.1°C. Negative contours are dashed.

Figure 4: Equatorial section of the mean spread of the ensembles of ocean initial conditions in a) FORCED, and b) 3DVAR. Isocontour interval is 0.1 °C.

Figure 5: Equatorial section of the mean linear response of the ensemble to perturbations in a) FORCED, and b) 3DVAR. Isocontour interval is 0.1°C. Negative contours are dashed.

Figure 6: Equatorial section of the mean spread of the ensembles of ocean initial conditions induced only by temperature perturbations only (members 4+ and 1-), in a) FORCED, and b) 3DVAR. Isocontour interval is 0.1°C.

Figure 7: Equatorial section of the mean spread of the ensembles of ocean initial conditions induced only by temperature and wind stress perturbations (members 2+ and 2-), in a) FORCED, and b) 3DVAR. Isocontour interval is 0.1°C.

Figure 8: Vertical profiles at a) 155°W and b) 95°W, of the innovation standard deviation in FORCED (bold solid line, circles) and 3DVAR (bold dashed line, circles), and of the ensemble spread in FORCED (thin solid line, squares) and 3DVAR (thin dashed line, squares). Note that the abscissa scale is different in a and b.

a)

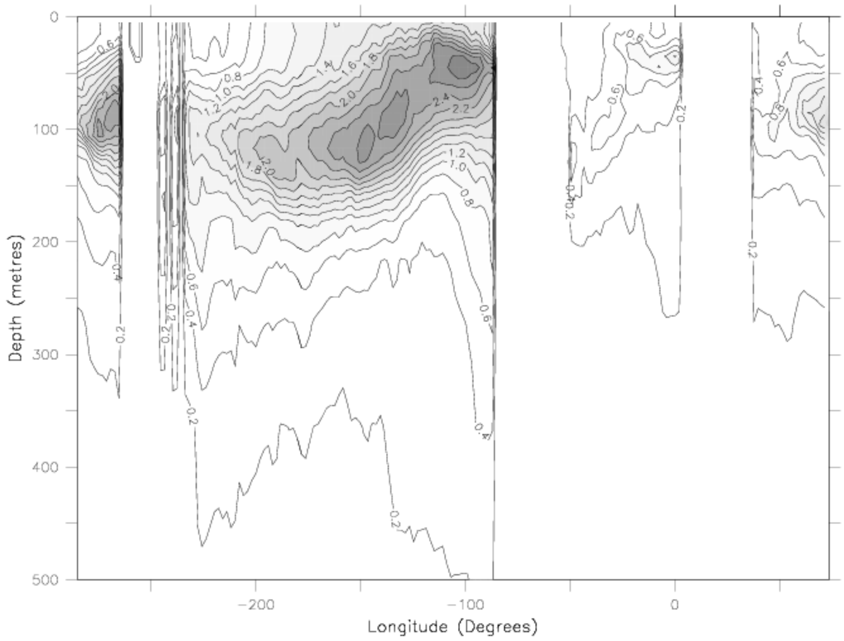

Depth (metres)
Longitude (Degrees)

b)

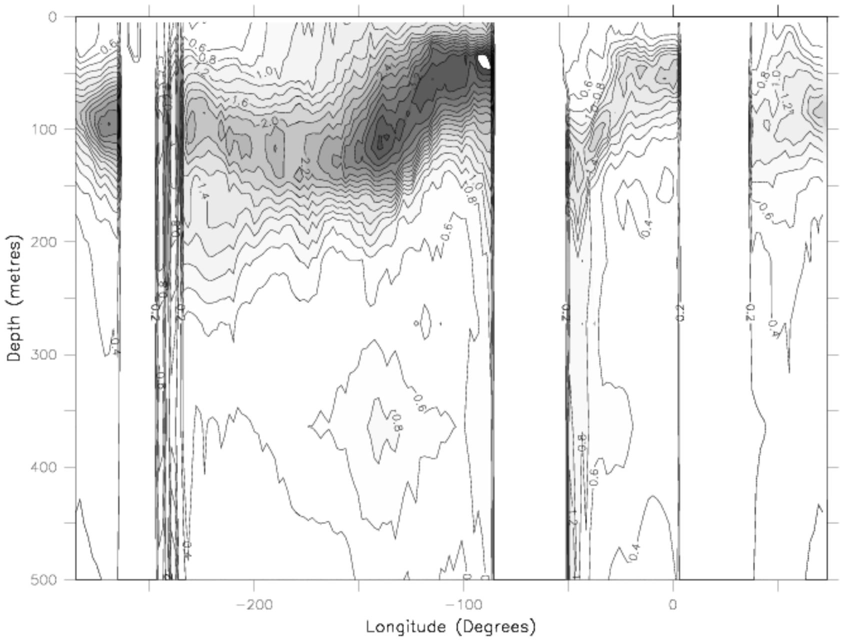

Depth (metres)
Longitude (Degrees)

Figure 1

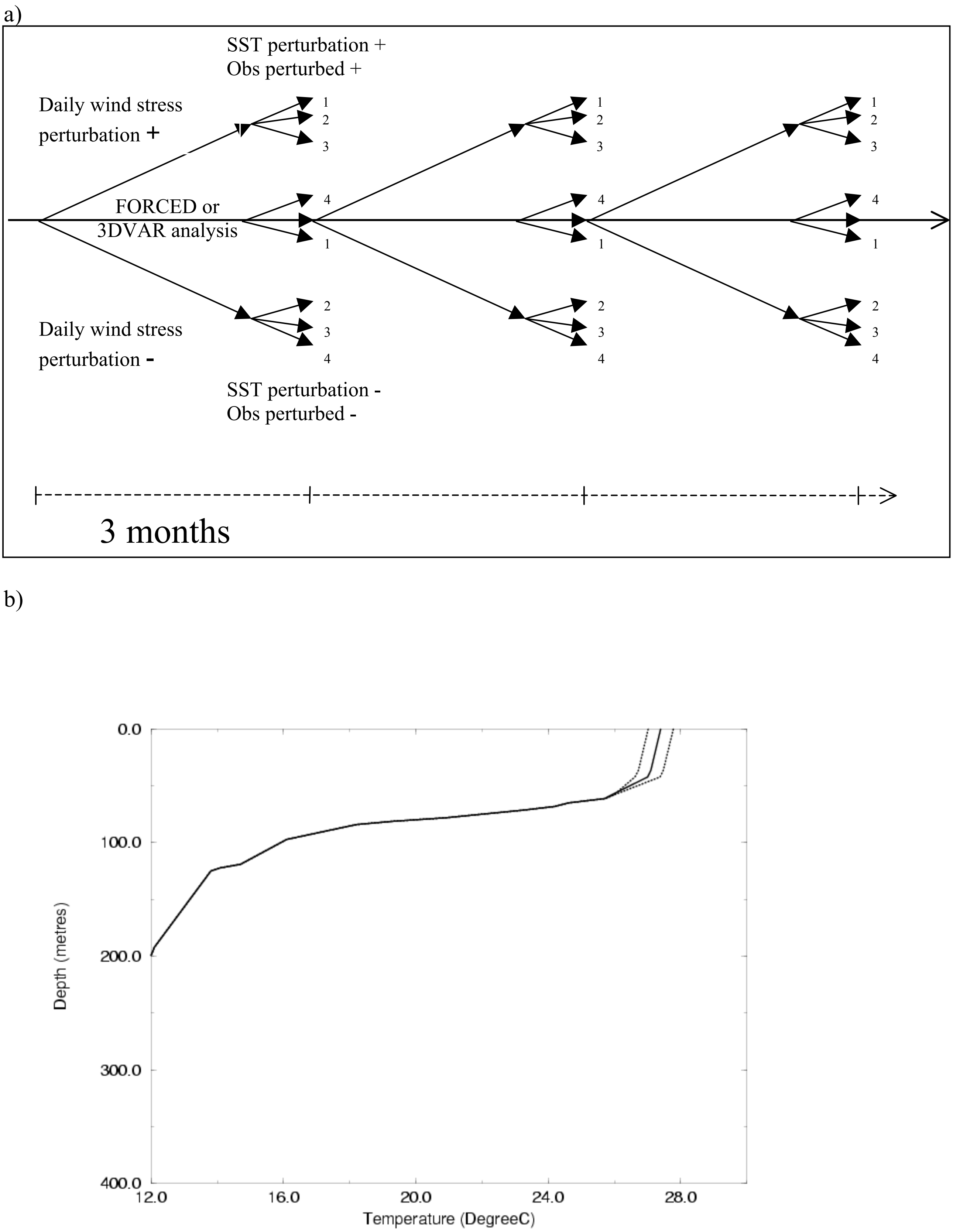
a)
SST perturbation +
Obs perturbed +
Daily wind stress
perturbation +
FORCED or
3DVAR analysis
Daily wind stress
perturbation -
SST perturbation -
Obs perturbed -
1
2
3
4
3 months
b)
0.0
100.0
200.0
300.0
400.0
Depth (metres)
12.0
16.0
20.0
24.0
28.0
Temperature (DegreeC)

Figure 2

a)

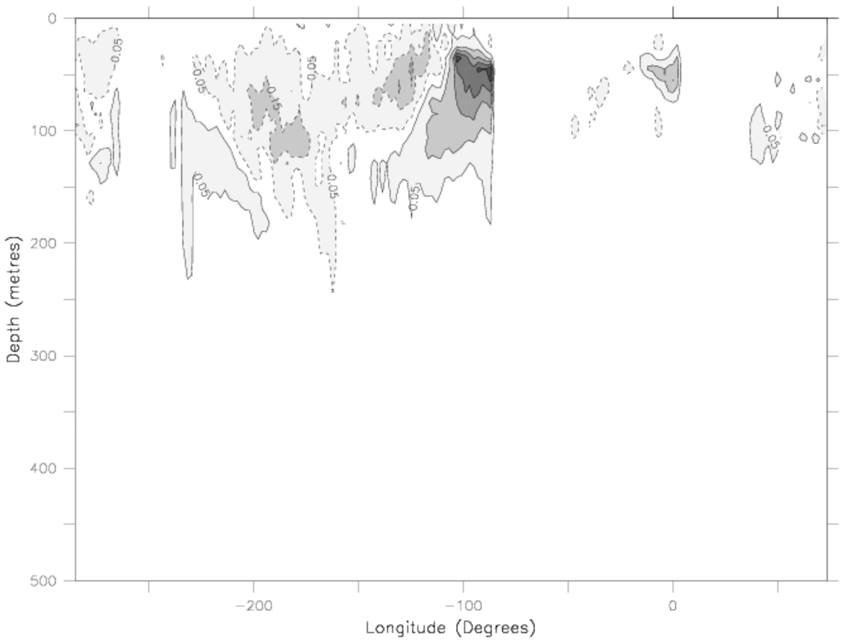

Depth (metres)
Longitude (Degrees)
0
100
200
300
400
500
-200
-100
0
-0.05
0.05

b)

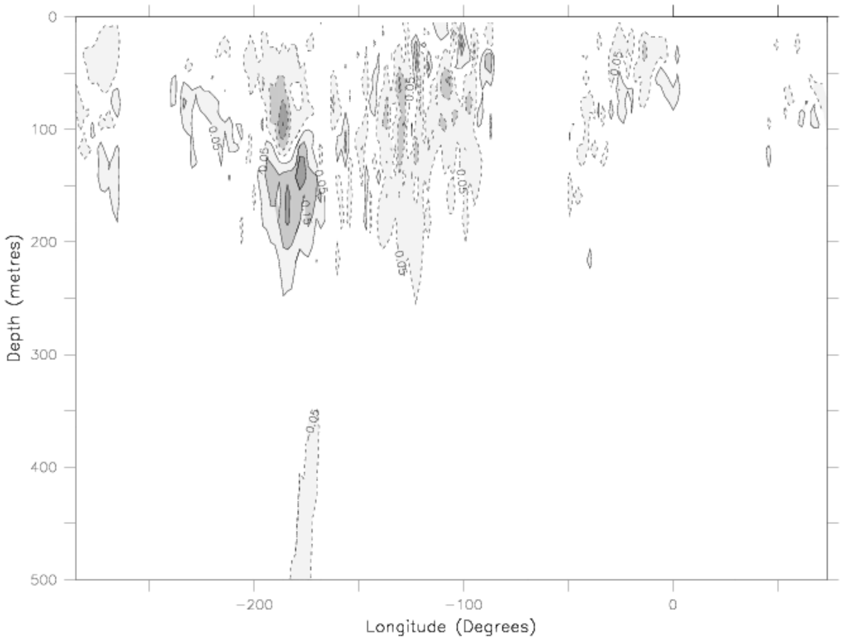

Depth (metres)
Longitude (Degrees)
0
100
200
300
400
500
-200
-100
0
-0.05
0.05

Figure 3

a)

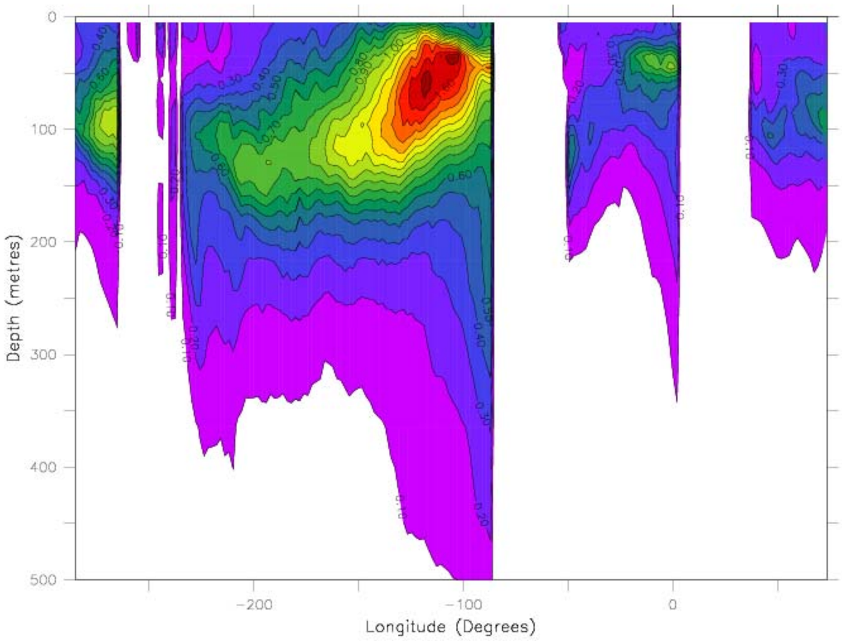

0
100
200
300
400
500
Depth (metres)
−200
−100
0
Longitude (Degrees)

b)

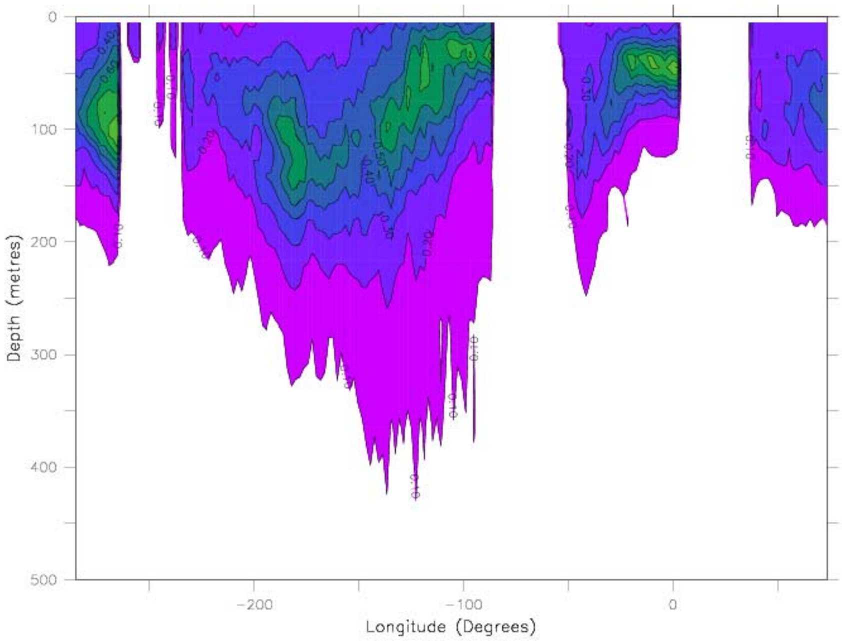

0
100
200
300
400
500
Depth (metres)
−200
−100
0
Longitude (Degrees)

Figure 4

a)

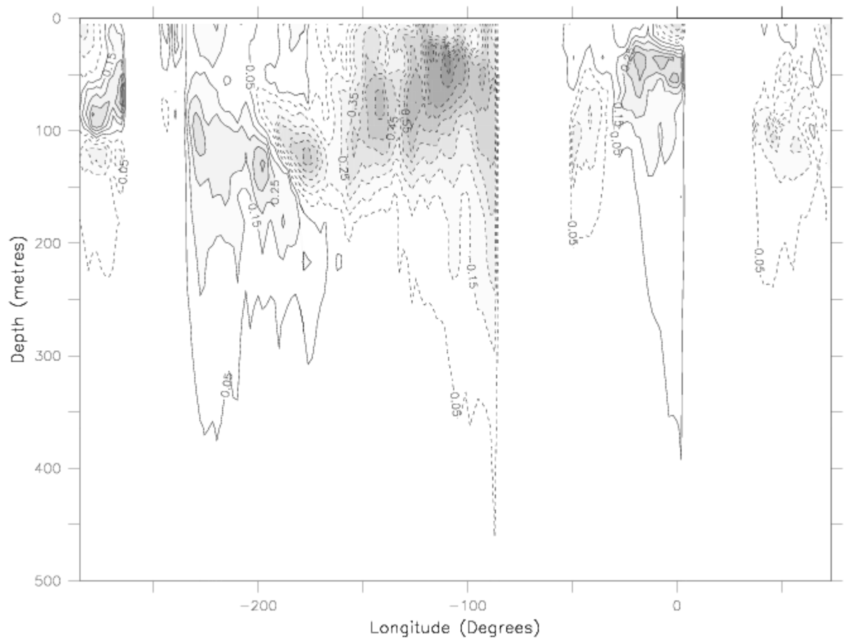

Depth (metres)
Longitude (Degrees)

b)

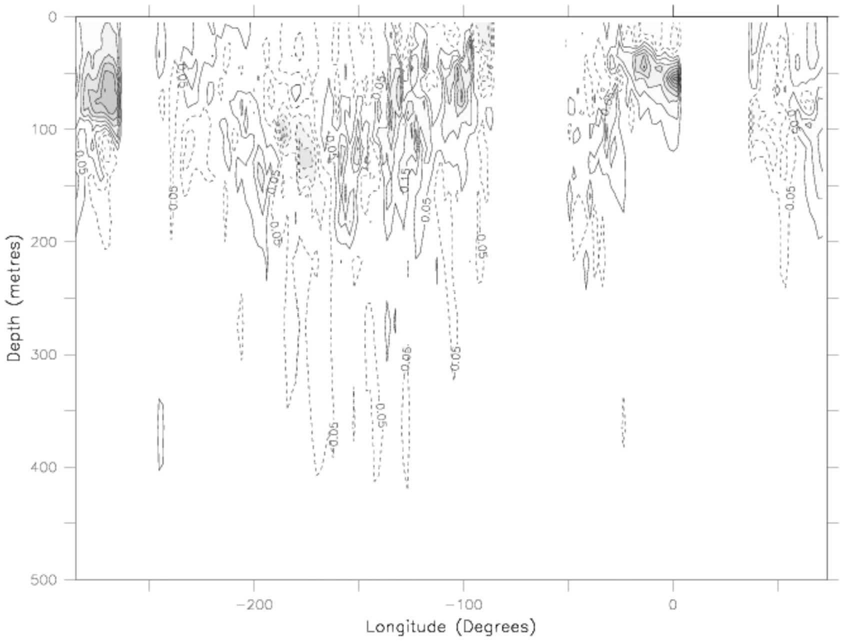

Depth (metres)
Longitude (Degrees)

Figure 5

a)

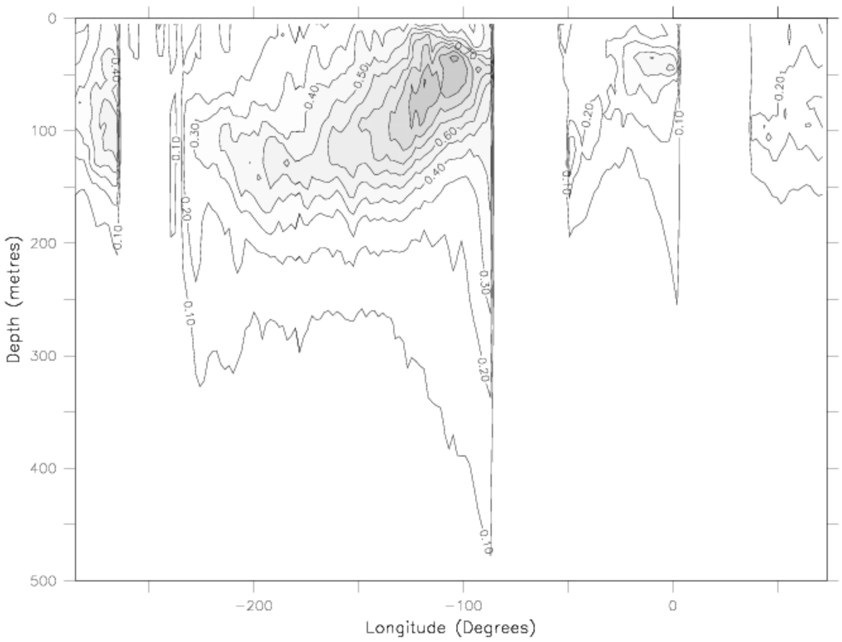

Depth (metres)
Longitude (Degrees)

b)

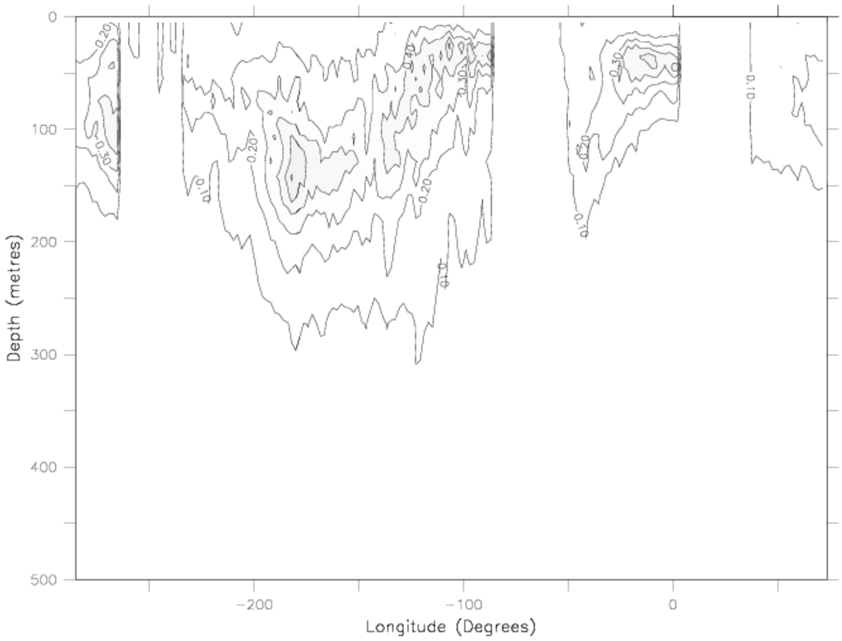

Depth (metres)
Longitude (Degrees)

Figure 6

a)

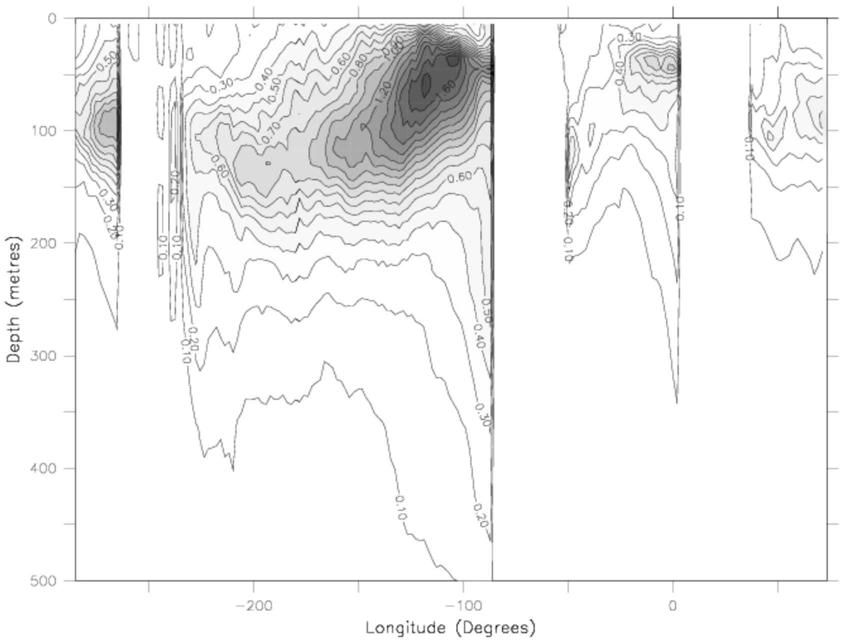
Depth (metres)
Longitude (Degrees)

b)

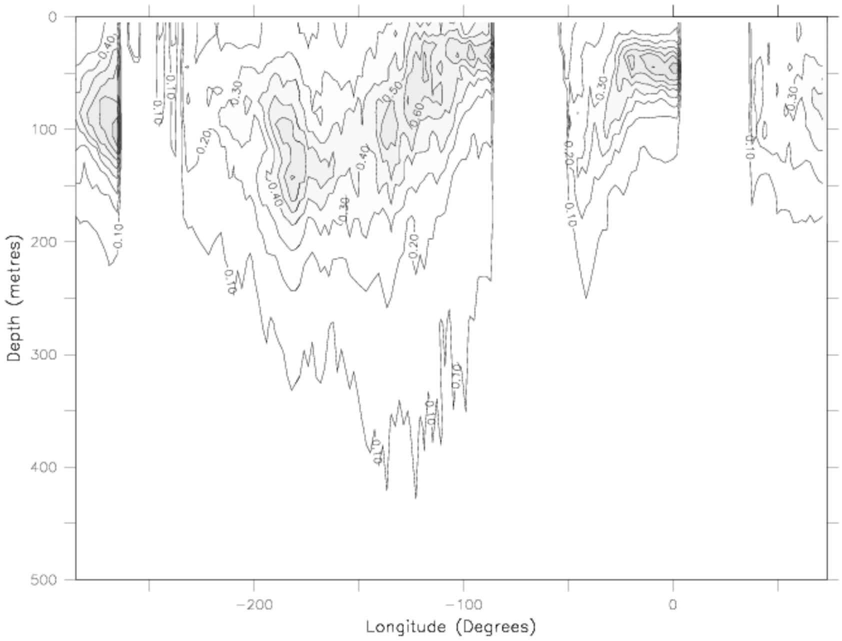
Depth (metres)
Longitude (Degrees)

Figure 7

a)

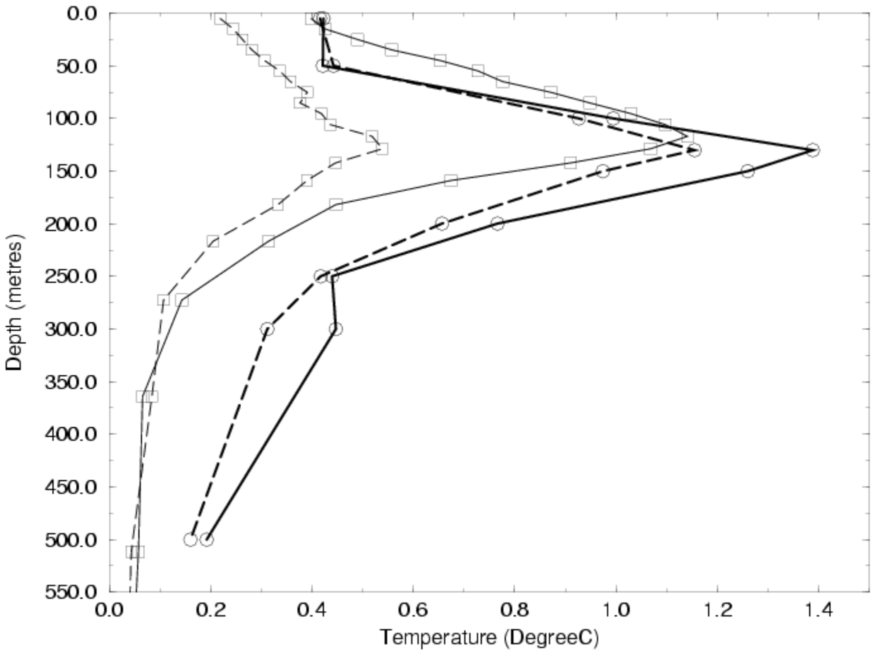
0.0
50.0
100.0
150.0
200.0
250.0
300.0
350.0
400.0
450.0
500.0
550.0
Depth (metres)
0.0
0.2
0.4
0.6
0.8
1.0
1.2
1.4
Temperature (DegreeC)

b)

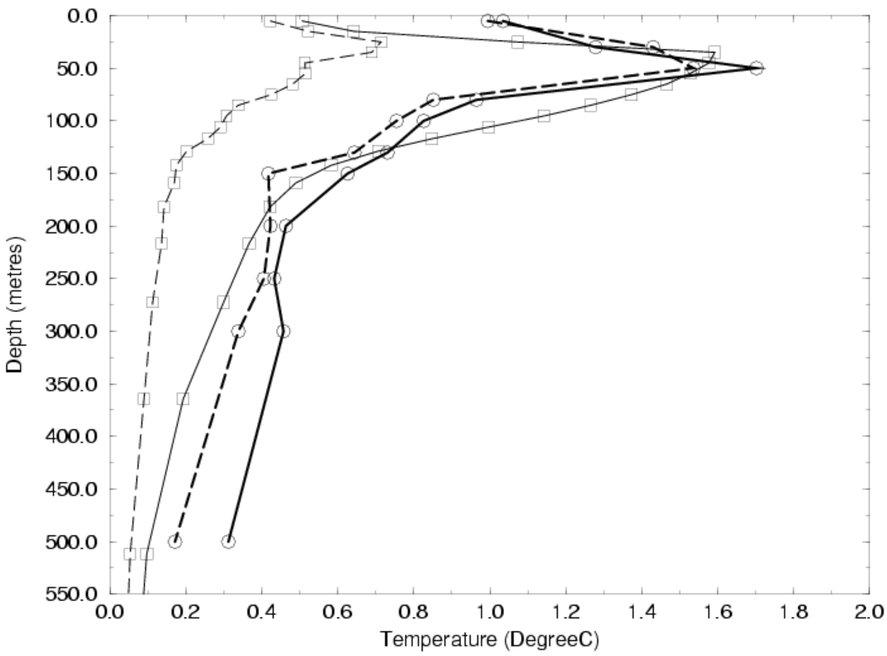
0.0
50.0
100.0
150.0
200.0
250.0
300.0
350.0
400.0
450.0
500.0
550.0
Depth (metres)
0.0
0.2
0.4
0.6
0.8
1.0
1.2
1.4
1.6
1.8
2.0
Temperature (DegreeC)

Figure 8